

Electron Spin Resonance Spin-Trapping Detection of Radical Intermediates in N-Doped TiO₂-Assisted Photodegradation of 4-Chlorophenol

Hongbo Fu, Liwu Zhang, Shicheng Zhang, and Yongfa Zhu*

Department of Chemistry, Tsinghua University, Beijing 100084, China

Jincai Zhao

Key Laboratory of Photochemistry, Institute of Chemistry, Chinese Academy of Sciences, Beijing 100080, China

Received: September 17, 2005; In Final Form: December 6, 2005

The electron spin resonance (ESR) spin-trapping technique using 5,5-dimethyl-1-pyrroline-*N*-oxide as the spin-trap reagent has been applied to detect free radical intermediates generated during in situ ultraviolet or visible irradiation of aqueous 4-chlorophenol (4-CP)/N-doped TiO₂ suspensions. ESR measurements gave the first direct evidence that the active species ([•]OH and O₂^{•-}) are responsible for the photodecomposition of 4-CP over N-doped TiO₂ under visible-light irradiation, strongly suggesting that the photocatalytic reaction of organic compounds in powdered N-doped TiO₂ systems proceed via surface intermediates of oxygen reduction or water oxidation, not via direct reaction with holes trapped at the N-induced midgap level. These results have important implications for the evaluation of the oxidative powder of TiO_{2-x}N_x catalysts.

Introduction

Various approaches have been attempted to enhance the visible-light utilization of TiO₂. Recently, the band gap of TiO₂ has been narrowed successfully by doping with nonmetal cations, by replacing lattice oxygen with B,¹ C,² N,³ or S^{4,5} dopants. It is widely recognized that anionic nonmetal dopants may be more appropriate for the extension of photocatalytic activity into the visible-light region, because the related impurity states are supposed to be close to the valence band maximum.⁶ Furthermore, the position of the conduction band minimum which must be kept at the level of the H₂/H₂O potential, when TiO₂ is used for the photocatalysis of water into hydrogen and oxygen, is not affected.⁶

Among all the nonmetal cations, substitutional N-doping was found to be particularly effective in decreasing the band gap of TiO₂ through mixing of N 2p and O 2p states. The presence of nitrogen doping extends the optical absorption of TiO₂ to the visible-light region and enhances visible-light-driven photocatalysis.^{7–16} The various N-doped TiO₂ catalysts have been applied to bleach methylene blue,⁷ split water,¹² and oxidatively degrade 2-propanol,¹⁴ 4-chlorophenol (4-CP),⁸ acetone vapors,¹⁶ and photokill harmful pathogens as well as peroxidation of the cell membrane of biomolecules.⁹ Indeed, visible-light-induced photocatalysis of N-doped TiO₂ is effective.

An open question is related to the photodegradation mechanism involved in N-doped TiO₂ photocatalysis. It has been reported that a variety of organic compounds are mineralized into CO₂ and inorganic species on N-doped TiO₂ under visible-light illumination.^{7,8,14} However, these studies do not distinguish whether the reaction product comes from a photooxidation process or a photoreduction process. It still remains conjectural whether a certain product comes from a direct reaction with photogenerated holes or via reactions with surface intermediates

of the water photooxidation reaction. It is thus quite difficult to get definite conclusions on the reaction mechanism. An examination of the formation of active oxygen species can provide useful information about the fate of the valence holes and the conduction electrons and lead to a greater understanding of visible-induced photocatalysis by N-doped TiO₂ in general. The electron spin resonance (ESR) technique offers an ideal method for the study of this type of interfacial photoreaction.^{17–19} A spin-trapping technique has been used to observe directly active radical intermediates in photoexcited TiO₂ aqueous suspensions and provides essential information for understanding the reaction mechanisms.^{20–22} However, to the best of our knowledge, for the N-doped TiO₂ system such meaningful work is still not reported.

We report here results involving spin-trapping of short-lived radical intermediates produced during in situ ultraviolet (UV) and visible irradiation of 4-CP/N-doped TiO₂ suspensions with a DMPO spin-trap reagent. The experimental results demonstrated the production of intermediates of hydroxyl (OH) and superoxide (O₂^{•-}) radicals in this photoprocess. The formation mechanism and the role of the radicals are discussed.

Experimental Section

5, 5-Dimethyl-1-pyrroline-*N*-oxide (DMPO) spin-trap reagent (Sigma Chemical Co.) was kindly supplied. Stock solutions of DMPO (0.4 M) in deaerated water were prepared under argon and stored in the dark at –20 °C. All chemicals were reagent grade and used without further purification. Deionized and doubly distilled water were used throughout this study.

N-Doped TiO₂ was prepared by the high-temperature nitridation of commercial P-25 (TiO₂, Degussa, 50 m² g⁻¹, 75% rutile and 25% anatase) as described by Irie et al.¹⁴ For comparison, the undoped sample was also annealed under N₂ in the same process as a reference sample. X-ray diffraction (XRD) patterns of the powders were recorded at room temperature by a Bruker D8 Advance X-ray diffractometer using Cu

* Corresponding author. Phone: +86-10-6278-7601. Fax: +86-10-6278-7601. E-mail: zhuyf@mail.tsinghua.edu.cn.

K α radiation and a 2θ scan rate of 2° min^{-1} . X-ray photoelectron spectroscopy (XPS) analysis was obtained using a PHI 5300 ESCA instrument with an Al K α X-ray source at a power of 250 W. The pass energy of the analyzer was set at 35.75 eV, and the base pressure of the analysis chamber was $<3 \times 10^{-9}$ Torr. The binding energy scale was calibrated with respect to the C 1s peak of hydrocarbon contamination fixed at 285.0 eV. According to Irie et al.,¹⁴ the peak at 396 eV is derived from Ti–N bonds. Therefore, the x values (nitrogen concentrations) in $\text{TiO}_{2-x}\text{N}_x$ were estimated by comparing to the product of the 396 eV peak area multiplied by the nitrogen-sensitive factor to the product of the 531 eV peak area (O 1s, Ti–O bonds) multiplied by the oxygen sensitivity factor. UV–visible diffuse reflectance (DR) spectra were obtained by using a Hitachi U-3010 spectrophotometer. BaSO_4 was the reference sample, and the spectra were recorded in the range 200–700 nm.

The photocatalytic activity of the as-prepared sample was evaluated by the decomposition of 4-CP when irradiated with UV light ($\lambda = 254 \text{ nm}$) and visible light ($\lambda > 420 \text{ nm}$). The UV light was obtained by a 12 W Hg lamp (Institute of Electric Light Source, Beijing), and the average light intensity was $50 \mu\text{W cm}^{-2}$. In the case of visible-light irradiation, a 500 W xenon lamp (Institute of Electric Light Source, Beijing) was focused through a window, and a 420 nm cutoff filter was placed onto the window face of the cell to ensure the desired irradiation light. The average light intensity was 30 mW cm^{-2} . The irradiation area was approximately 40 cm^2 . The radiant flux was measured with a power meter from the Institute of Electric Light Source (Beijing, China). Aqueous suspensions of 4-CP (usually 100 mL, 10 mg L^{-1}) and 0.1 g of the catalysts were placed in a vessel. Prior to irradiation, the suspensions were magnetically stirred in dark for ca. 30 min to ensure the establishment of an adsorption/desorption equilibrium. The suspensions were kept under constant air-equilibrated conditions before and during the irradiation. At given time intervals, 3 mL aliquots were sampled and centrifuged to remove the particles. The filtrates were analyzed by recording variations in the absorption band (224 nm) in the UV–visible spectra of 4-CP using a Hitachi U-3010 spectrophotometer.

ESR signals of radicals spin-trapped by DMPO were recorded at ambient temperature on a Bruker ESR 300 E spectrometer: the irradiation source was a Quanta-Ray Nd:YAG pulsed laser system ($\lambda = 355$ or 532 nm , 10 Hz). The settings for the ESR spectrometer were as follows: center field, 3486.70 G; sweep width, 100 G; microwave frequency, 9.82 GHz; modulation frequency, 100 kHz; power, 5.05 mW. To minimize experimental errors, the same quartz capillary tube was used for all ESR measurements. The ESR spectrometer was coupled to a computer for data acquisition and instrument control. Magnetic parameters of the radicals detected were obtained from direct measurements of magnetic field and microwave frequency.

Results and Discussion

The XRD pattern of N-doped TiO_2 shows that replacing an O atom with an N atom in TiO_2 does not result in significant structural changes, although the N atom has a larger ionic radius (0.171 nm) than that of the O atom (0.132 nm).¹³ The Ti–N bond length, 1.964 Å, is only slightly longer than that of Ti–O, 1.942 Å. Therefore, the structural modifications due to N doping are relatively minor. A new peak at 396 eV was observed from the XPS spectrum of the N-doped sample, which is generally considered as evidence for the presence of Ti–N bonds, suggesting that the oxygen sites were substituted by nitrogen atoms.²⁶ Therefore, the N-doped sample could be

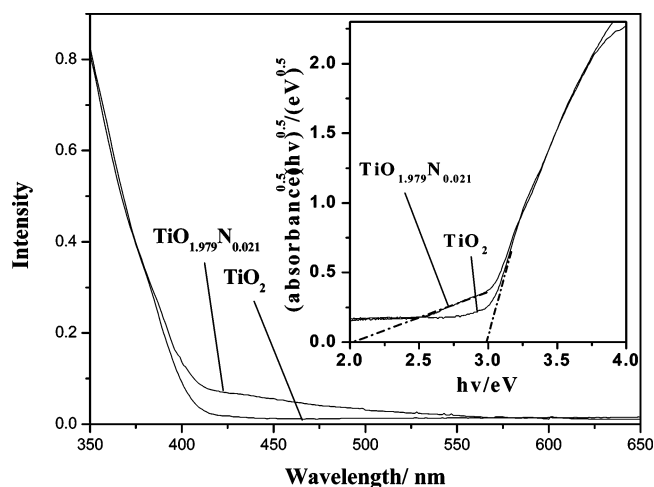


Figure 1. UV–visible reflectance spectra of TiO_2 and $\text{TiO}_{1.979}\text{N}_{0.021}$.

described as $\text{TiO}_{2-x}\text{N}_x$, where the x value was estimated to be 0.021 from the XPS spectrum. In contrast, the N_2 gas annealed samples did not display a peak at 396 eV and was TiO_2 .

Figure 1 shows UV–visible DR spectra of $\text{TiO}_{1.979}\text{N}_{0.021}$ and TiO_2 . A noticeable shift of the absorption shoulder into the visible-light region was observed for $\text{TiO}_{1.979}\text{N}_{0.021}$. This absorption shoulder at 400–550 nm is related to the presence of nitrogen, which well agrees with the reported value for the N-doped TiO_2 system.^{8,13} It is noted that the N-doping did not cause a shift of the absorbance edge of TiO_2 , which could be due to the low amount of N-doping ($x = 0.021$). We concluded that the visible light response for $\text{TiO}_{1.979}\text{N}_{0.021}$ could arise from an N-induced midgap level, formed above the valence band (O 2p).¹⁴ TiO_2 is an indirect gap semiconductor, and the band gaps of $\text{TiO}_{1.979}\text{N}_{0.021}$ and TiO_2 can be estimated from tangent lines in the plots of the square root of the Kubelka–Munk functions against the photon energy,^{14,23} as shown in the inset of Figure 1. The tangent lines, which are extrapolated to $\alpha^{1/2} = 0$, indicate the band gaps of $\text{TiO}_{1.979}\text{N}_{0.021}$ and TiO_2 are $E_g = 3.0 \text{ eV}$. The N-induced midgap of $\text{TiO}_{1.979}\text{N}_{0.021}$ could be roughly estimated to be 2.0 eV from the inset. The doped sample is pale-yellow in color, whereas the undoped sample is white. The color of the N-doped sample may be partially due to the bulk reduction of the crystal, because the thermal decomposition of NH_3 on the TiO_2 surface results in the evolution of molecular hydrogen, which reduces the crystal electronically.⁶ In addition, the presence of a visible absorption band indicates that nitrogen penetrates into the single crystal and effectively changes the electronic structure of TiO_2 .^{6,14}

To explore the photocatalytic activity of the as-prepared sample, the degradation of 4-CP was investigated using both UV and visible irradiation. 4-CP does not absorb in the visible region, and therefore the presence of indirect semiconductor photocatalysis can be excluded.⁸ Figure 2A shows the changes of 4-CP concentration as a function of time in the presence of $\text{TiO}_{1.979}\text{N}_{0.021}$ powder under UV irradiation. Almost no degradation occurred in the case of UV irradiation alone. TiO_2 exhibited a higher activity for 4-CP decomposition than that of $\text{TiO}_{1.979}\text{N}_{0.021}$. A 59% loss of 4-CP in concentration was observed in the presence of TiO_2 for a 2 h irradiation. The somewhat decreased photoactivity of N-doped TiO_2 could result as the doped N atoms act as a recombination center of photogenerated charge carriers and thus deteriorate the activity of the catalyst.¹⁴ Similar experiments were conducted under visible-light irradiation. The results are shown in Figure 2B. Irradiating TiO_2 with visible light did not generate a decrease of 4-CP in concentration, as it

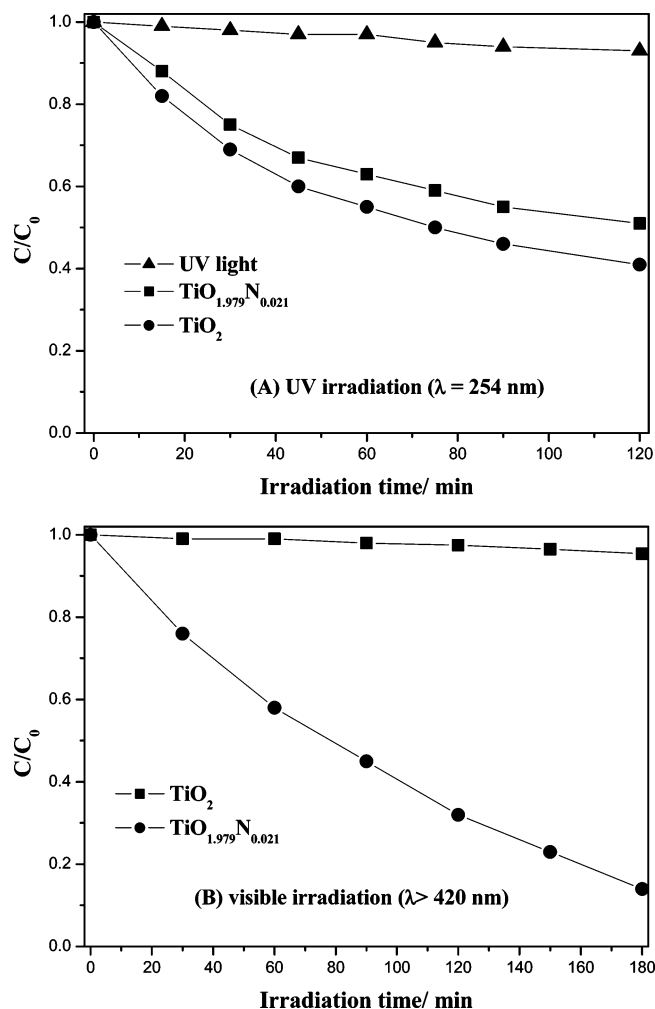


Figure 2. Photodecomposition of 4-CP by TiO_2 and $\text{TiO}_{1.979}\text{N}_{0.021}$ under UV light (A) and visible light (B): catalyst loading, 0.5 g L^{-1} ; 4-CP concentration, 10 mg L^{-1} .

was not visible-light sensitive. The degradation of 4-CP, however, was observed from $\text{TiO}_{1.979}\text{N}_{0.021}$, suggesting that N doping for TiO_2 is an effective and feasible approach for achieving visible-light-driven photocatalysis.

We employed the ESR spin-trap technique (with DMPO), a useful method to monitor intermediate radicals, to probe the nature of the reactive oxygen species generated during the irradiation of the present system. The experiments were first carried out under UV irradiation, and the results are shown in Figure 3. No ESR signals were observed either when 4-CP was absent or when the reaction was performed in the dark in the presence of the catalysts. Under UV irradiation the characteristic quartet peaks of the DMPO- OH adduct with a 1:2:2:1 intensity observed after a 20 s preillumination period, consist with the similar spectra reported by others for the $\cdot\text{OH}$ adduct.²⁴ The intensity of the peaks further increased with 80 s of irradiation. Under the same experiment conditions, the peak intensity of $\cdot\text{OH}$ generated by $\text{TiO}_{1.979}\text{N}_{0.021}$ was less than that of TiO_2 , suggesting a lower production of $\cdot\text{OH}$.

Although the formation of the superoxide radical anion was expected owing to the scavenging of electrons by O_2 , because N doping did not affect the conduction band of TiO_2 ,⁶ the spin-adduct $\text{DMPO}-\cdot\text{OOH}/\text{O}_2^{\cdot-}$ was not detected in the aqueous system. It is well documented that the superoxide radical anions are produced first and remain stable in an organic solvent medium (at least in methanol).²⁵ When the fraction of H_2O is increased, such as occurs in a $\text{CH}_3\text{OH}/\text{H}_2\text{O}$ mixed solvent

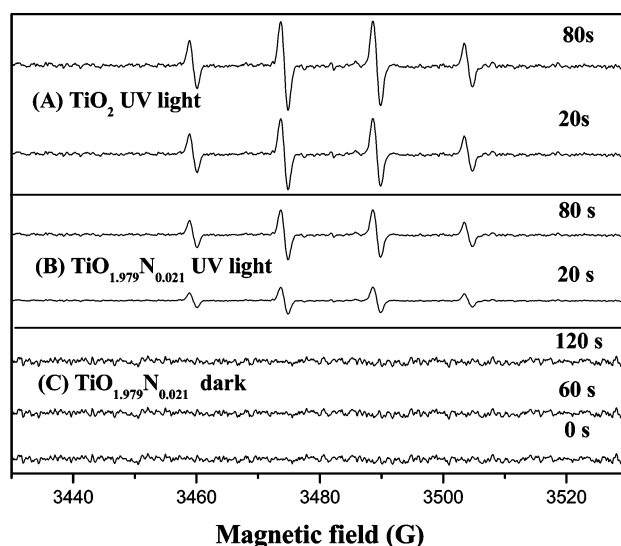


Figure 3. DMPO spin-trapping ESR spectra under UV irradiation in 4-CP/ $\text{TiO}_{1.979}\text{N}_{0.021}$ aqueous solutions: catalyst loading, 0.5 g L^{-1} ; 4-CP concentration, 10 mg L^{-1} ; DMPO concentration, $1.6 \times 10^{-2} \text{ M}$.

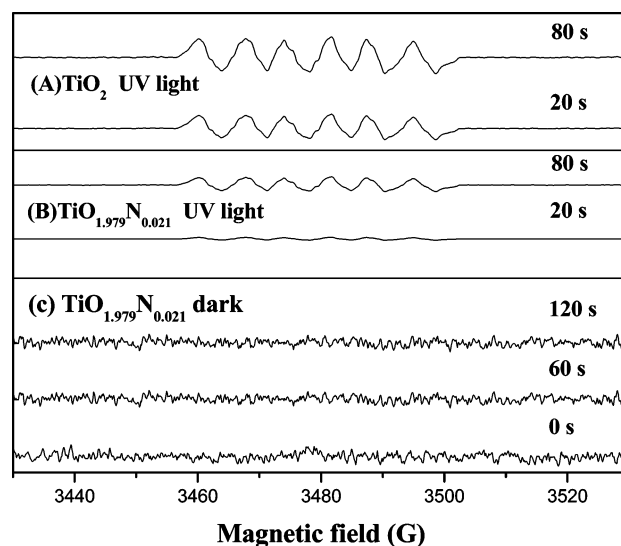


Figure 4. DMPO spin-trapping ESR spectra under UV irradiation in 4-CP/ $\text{TiO}_{1.979}\text{N}_{0.021}$ ethanol solutions: catalyst loading, 0.5 g L^{-1} ; 4-CP concentration, 10 mg L^{-1} ; DMPO concentration, $1.6 \times 10^{-2} \text{ M}$.

system, the superoxide radical anion tends to be unstable, especially in H_2O alone. $\text{O}_2^{\cdot-}$ readily converted to H_2O_2 and O_2 ($2\text{O}_2^{\cdot-} + 2\text{H}^+ \rightarrow \text{O}_2 + \text{H}_2\text{O}_2$, $k = 6.6 \times 10^3 \text{ M}^{-1} \text{ s}^{-1}$). It is probably because the facile disproportionation reaction of the superoxide in water precludes the slow reactions between $\cdot\text{OOH}/\text{O}_2^{\cdot-}$ and DMPO ($k = 10 \text{ M}^{-1} \text{ s}^{-1}$).²⁶ Consequently, we recorded the ESR spectra of the DMPO- $\cdot\text{OOH}/\text{O}_2^{\cdot-}$ spin adducts in methanolic media, and the results are as shown in Figure 4. The six characteristic peaks of the $\cdot\text{OOH}/\text{O}_2^{\cdot-}$ adducts were observed under UV irradiation, and the signal intensity increased slightly with irradiation time. No such signals were observed in the dark; that is, generation of $\text{O}_2^{\cdot-}$ anions in the N-doped TiO_2 system inherently implicates irradiation. Compared to the ESR signals of $\cdot\text{OOH}/\text{O}_2^{\cdot-}$ in TiO_2 , the signals of $\cdot\text{OOH}/\text{O}_2^{\cdot-}$ were less intense in the case of $\text{TiO}_{1.979}\text{N}_{0.021}$, suggesting the lower production of $\text{O}_2^{\cdot-}$.

ESR signals were then measured for the 4-CP/ $\text{TiO}_{1.979}\text{N}_{0.021}$ systems with visible-light irradiation. The ESR signal of the DMPO- $\cdot\text{OH}$ adducts in water solution and DMPO- $\cdot\text{OOH}/\text{O}_2^{\cdot-}$ adducts could be observed, and the ESR signal intensity was

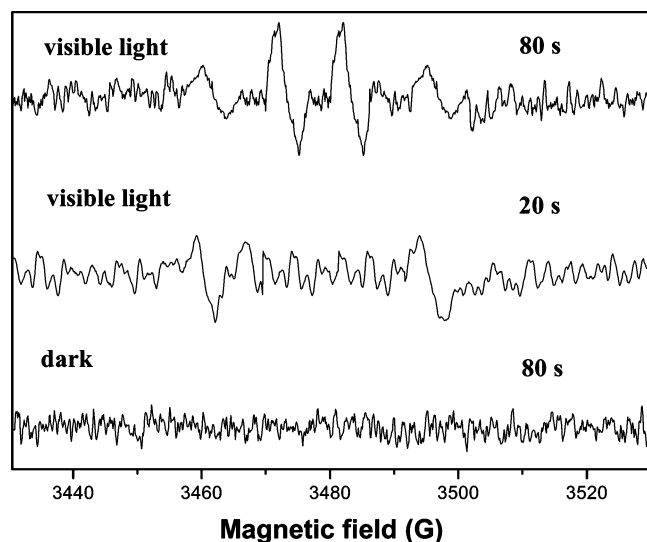


Figure 5. DMPO spin-trapping ESR spectra under visible irradiation in 4-CP/TiO_{1.979}N_{0.021} aqueous solutions: catalyst loading, 0.5 g L⁻¹; 4-CP concentration, 10 mg L⁻¹; DMPO concentration, 1.6 × 10⁻² M.

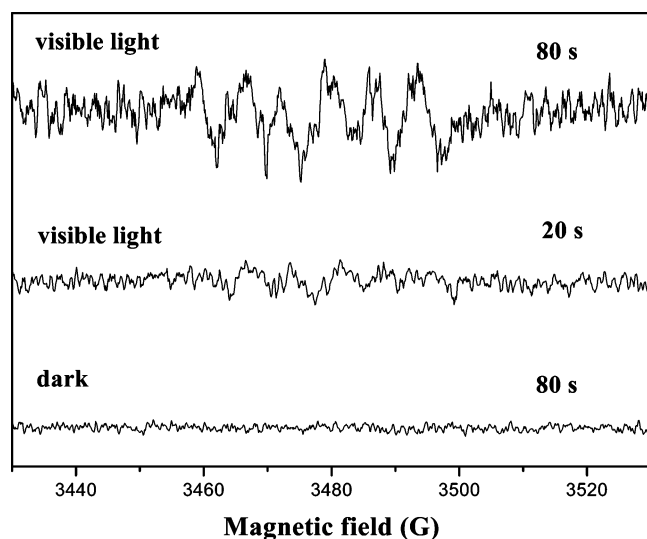
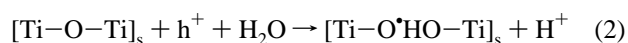


Figure 6. DMPO spin-trapping ESR spectra under visible irradiation in 4-CP/TiO_{1.979}N_{0.021} ethanol solutions: catalyst loading, 0.5 g L⁻¹; 4-CP concentration, 10 mg L⁻¹; DMPO concentration, 1.6 × 10⁻² M.

enhanced gradually with increasing illumination time. The results are shown in Figure 5 and Figure 6, respectively. The experimental results are the same as that for UV irradiation. No ESR signals were observed in the dark under otherwise identical conditions as those for the visible photoreaction. This clarifies that the degradation of 4-CP over N-doped TiO₂ occurs mainly by the radical reaction, which is similar to TiO₂ under UV light irradiation.

In most of the proposed mechanisms of the photocatalytic degradations of organic pollutants mediated by semiconductors, the highly oxidizing (surface-bound) hydroxyl radical, which originates from the oxidation of chemisorbed OH⁻ or H₂O by photogenerated valence band holes, is regarded as the main oxidative species responsible for the degradation.²⁷ No doubt some reactions can also be initiated by direct hole oxidation, especially when the adsorption by the substrates is rather extensive and the concentrations of substrates are relatively high.²⁸ In the present study, ESR measurements for the first time give direct evidence that the active species ([•]OH and O₂^{•-}) are responsible for the photodecomposition of 4-CP, strongly suggesting that the photocatalytic reaction of organic compounds

in powdered N-doped TiO₂ system proceed via surface intermediates of oxygen reduction or water oxidation, not via direct reactions with holes trapped at the N-induced midgap level. Colussi et al.²⁹ have insisted that N-doped TiO₂ could not efficiently catalyze the photooxidation of typical aqueous organic contaminants. By a detailed potential level analysis, they concluded that the N-doped TiO₂ suspension with visible-light irradiation did not produce oxidizing species powerful enough to oxidize the organic pollutants. As for the N-doped sample prepared in the present work, the isolated narrow band formed by N doping above the valence band could be responsible for the visible-light response. Irradiation with UV light excites electrons from both the O 2p and the N 2p orbitals formed by the N doping to the Ti 3d orbitals, but irradiating with visible light only excites electrons from the isolated N 2p orbitals to the Ti 3d orbitals. Indeed, the N-induced midband of TiO_{1.979}N_{0.021} is about 2.0 eV (the insert of Figure 1), which is critically close to the potential of [•]OH/OH⁻ (+1.99).²⁹ From this viewpoint, a strong oxidizing species could not be produced in the N-doped TiO₂ suspension under visible-light irradiation. Apparently, this is not in agreement with our ESR measurements. This pivotal question could be explained if we take into account that the water oxidation is not caused by an electron-transfer type reaction. Very recently, Nakato et al.^{30,31} reported that the water photooxidation on *n*-TiO₂ is not induced by the oxidation of a surface OH group (Ti—OH_s) with photogenerated holes (h⁺) (eq 1), which was commonly considered the initiation step of the oxygen photoevolution reaction on TiO₂. It could be initiated by a nucleophilic attack of an H₂O molecule (Lewis base) to a surface-trapped hole (Lewis acid) at a surface lattice O site accompanied by bond breaking (eq 2). Their conclusion is supported by photoluminescence measurements.³¹ It is worth noting here that reaction 1 is an electron-transfer-type reaction, whereas reaction 2 is a Lewis acid–base-type reaction, and therefore their energetic and kinetics are quite different from each other.³¹



Reaction 2 is easily realized and will not have any direct relation with the redox potential such as *E*_{eq} ([•]OH/H₂O) but will have a strong relation with the basicity of H₂O or the energy of the intermediate radical [Ti—O HO—Ti]_s that is roughly giving the activation for the reaction.³¹ The suggestion of water photooxidation gives strong support for the generation of [•]OH in the present study.

Acknowledgment. This work was partly supported by the Chinese National Science Foundation (20433010, 20571047) and Trans-Century Training Program Foundation for the Talents by the Ministry of Education, People's Republic of China, and China Postdoctoral Science Foundation.

Supporting Information Available: XRD patterns and X-ray photoelectron spectra of TiO₂ and N-doped TiO₂. This material is available free of charge via the Internet at <http://pubs.acs.org>.

References and Notes

- (1) Zhao, W.; Ma, W.; Chen, C.; Zhao, J.; Shuai, Z. *J. Am. Chem. Soc.* **2004**, *126*, 4782.
- (2) Khan, S.; Shahry, M.; Ingler, W. B. *Science* **2002**, *297*, 2243.

- (3) Asahi, R.; Morikawa, T.; Ohwaki, T.; Aoki, K.; Taga, Y. *Science* **2001**, 293, 269.
- (4) Ohno, T.; Mitsui, T.; Matsumura, M. *Chem. Lett.* **2003**, 32, 364.
- (5) Yu, J. C.; Ho, W.; Yu, J.; Yip, H.; Wong, P.; Zhao, J. *Environ. Sci. Technol.* **2005**, 39, 1175.
- (6) Diwald, O.; Thompson, T. L.; Zubkov, T.; Goralski, Ed. G.; Walck, S. D.; Yates, J. T., Jr. *J. Phys. Chem. B* **2004**, 108, 6004.
- (7) Gole, J. L.; Stout, J. D. *J. Phys. Chem. B* **2004**, 108, 1230.
- (8) Sakthivel, S.; Janczarek, M.; Kisch, H. *J. Phys. Chem. B* **2004**, 108, 19384.
- (9) Bacsa, R.; Kiwi, J.; Ohno, T.; Albers, P.; Nadtochenko, V. *J. Phys. Chem. B* **2005**, 109, 1384.
- (10) Hong, X.; Wang, Z.; Cai, W.; Lu, F.; Zhang, J.; Yang, Y.; Ma, N.; Liu, Y. *Chem. Mater.* **2005**, 17, 1548.
- (11) Burda, C.; Lou, Y.; Chen, X.; Samia, A. C. S.; Stout, J.; Gole, J. L. *Nano Lett.* **2003**, 3, 1049.
- (12) Toorres, G. R.; Lindgren, T.; Lu, J.; Granqvist, C.-G.; Lindquist, S.-E. *J. Phys. Chem. B* **2004**, 108, 5995.
- (13) Li, D.; Haneda, H.; Hishita, S.; Ohashi, N. *Chem. Mater.* **2005**, 17, 2588.
- (14) Irie, H.; Watanabe, Y.; Hashimoto, K. *J. Phys. Chem. B* **2003**, 107, 5483.
- (15) Chen, X.; Burda, C. *J. Phys. Chem. B* **2004**, 108, 9867.
- (16) Khan, S. U. M.; Al-Shahry, M.; Ingler, W. B., Jr. *Science* **2002**, 297, 2243.
- (17) Hirakawa, T.; Kominami, H.; Ohtani, B.; Nosaka, Y. *J. Phys. Chem. B* **2001**, 105, 6993.
- (18) Liu, G.; Zhao, J.; Hidaka, H. *J. Photochem. Photobiol., A* **2000**, 133, 83.
- (19) Li, J.; Ma, W.; Huang, Y.; Tao, X.; Zhao, J.; Xu, Y. *Appl. Catal., B* **2004**, 48, 17.
- (20) Qu, P.; Zhao, J.; Shen, T.; Hidaka, H. *J. Mol. Catal. A: Chem.* **1998**, 129, 527.
- (21) Wu, T.; Lin, T.; Zhao, J. *Environ. Sci. Technol.* **1999**, 33, 1379.
- (22) Chen, C.; Li, X.; Ma, W.; Zhao, J. *J. Phys. Chem. B* **2002**, 106, 318.
- (23) Domen, K.; Kudo, A.; Onishi, T. *J. Catal.* **1986**, 10, 217.
- (24) Huang, Y.; Li, J.; Ma, W.; Cheng, M.; Zhao, J. *J. Phys. Chem. B* **2004**, 108, 7263.
- (25) Chen, C.; Zhao, W.; Lei, P.; Zhao, J.; Serpone, N. *Chem. Eur. J.* **2004**, 10, 1956.
- (26) Liu, G.; Li, X.; Zhao, J. *Environ. Sci. Technol.* **2000**, 34, 3982.
- (27) Hoffmann, M. R.; Martin, S. T.; Choi, W. *Chem. Rev.* **1995**, 95, 69.
- (28) Kim, S.; Park, H.; Choi, W. *J. Phys. Chem. B* **2004**, 108, 6402.
- (29) Mrowetz, M.; Balcerski, W.; Colussi, A. J.; Hoffmann, M. R. *J. Phys. Chem. B* **2004**, 108, 17270.
- (30) Nakamura, R.; Tanaka, T.; Nakato, Y. *J. Phys. Chem. B* **2004**, 108, 10617.
- (31) Nakamura, R.; Nakato, Y. *J. Am. Chem. Soc.* **2004**, 126, 1290.